Molecular Crystals and Liquid Crystals Science and Technology. Section A. Molecular Crystals and Liquid Crystals

Publication details, including instructions for authors and subscription information:
http://www.tandfonline.com/loi/gmcl19

Low and High Frequency Relaxations of a Ferroelectric Liquid Crystal

M. R. De La Fuente [a], S. Merino [a], M. A. Pérez Jubindo [a] & T. Sierra [b]

[a] Departamentode Física Aplicada II, F. Ciencias, Universidad del País Vasco Apdo. 644, 48080, Bilbao, Spain

[b] Departamento de Química Orgánica, Facultad de Ciencias, Institute de Ciencia tie Materiales de Aragón, Universidad de Zaragoza-C. S.I.C, 50009, Zaragoza, Spain

Version of record first published: 23 Sep 2006.

To cite this article: M. R. De La Fuente , S. Merino , M. A. Pérez Jubindo & T. Sierra (1995): Low and High Frequency Relaxations of a Ferroelectric Liquid Crystal, Molecular Crystals and Liquid Crystals Science and Technology. Section A. Molecular Crystals and Liquid Crystals, 259:1, 1-12

To link to this article: http://dx.doi.org/10.1080/10587259508038668

Mol. Cryst. Liq. Cryst., 1995, Vol. 259, pp. 1–12
Reprints available directly from the publisher
Photocopying permitted by license only

Low and High Frequency Relaxations of a Ferroelectric Liquid Crystal

M. R. DE LA FUENTE, S. MERINO and M. A. PÉREZ JUBINDO

Departamento de Física Aplicada II, F. Ciencias, Universidad del País Vasco Apdo. 644, 48080, Bilbao, Spain

T. SIERRA

Departamento de Química Orgánica, Facultad de Ciencias, Instituto de Ciencia de Materiales de Aragón, Universidad de Zaragoza-C. S.I.C, 50009 Zaragoza Spain

(Received June 7, 1994)

Broadband dielectric measurements on a ferroelectric liquid crystal have been carried out. The alignment was planar and the cell and sample holder were the same in the whole frequency range. Five different relaxations have been obtained and characterized: soft mode, Goldstone mode, molecular reorientation around the transversal axis, molecular reorientation around the longitudinal axis and a ferroelectric domain mode. Strengths and frequencies of these modes have been obtained in the different phases for different bias fields.

INTRODUCTION

Dielectric spectroscopy is a powerful tool to study the dynamics of liquid crystals. Molecular and phase anisotropy, individual and collective molecular motions, and structural organization are only some of the properties that could be studied by broadband dielectric measurements. In the case of ferroelectric liquid crystals (FLC), low frequency dielectric spectroscopy (10^2–10^6 Hz) has been extensively used to study the amplitude (soft mode) and phase (Goldstone mode) fluctuations of the director.[1–8] More recently, the high frequency range (10^6–10^9 Hz) has been acquiring an increasing interest related to the study of molecular reorientation around the long axis in the para-ferroelectric SmA-SmC* phase transition.[9–12] This point has also been studied by means of *degenerate four-wave-mixing experiments*[13] and *transient optical Kerr experiments.*[14] After some controversy, it seems that this motion does not show, any pretransitional characteristic nor any slowing down. As a result the appearence of the ferroelectricity in the SmC* phase is not related to the freezing of this motion. In addition, studies on non-chiral liquid crystals with SmA-SmC transition show the same behaviour.

In this paper we report broadband dielectric spectroscopy sudies in the FLC: 2′-[6′-((2″S,3″S-2″-chloro-3″-methylpentanoyl)oxy)] naphthyl-4-decyloxybenzoate which exhibits the phase sequence I-N*-SmA-SmC*. Previous molecular mechanic empirical calculations (MM2)[15] shows that this compound, with the chlorine

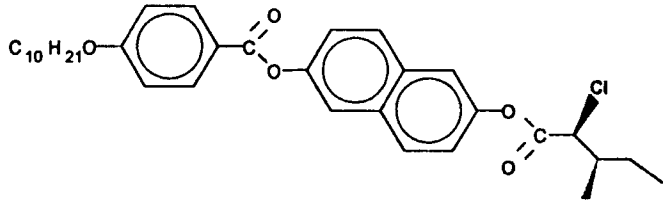

2'-[8'-((2"S,3"S-2"-chloro-3"-methylpentanoyl)oxy)]-naphthyl-4-n-decyloxybenzoate

atom in one of the chiral centers, has an important bulky alkyl group, this steric factor being very important in the molecular arrangement in the SmC* phase and thus in the value of the spontaneous polarization. The alignment was planar and we have observed many different dielectrically-active modes: Goldstone, and soft modes, molecular modes and a type of structural mode related to domains in the ferroelectric phase. Amplitudes, frequencies and activation energies of the different modes in all mesophases have been determined from the dielectric response in the frequency range 100 Hz to 1 GHz with different conditions for a bias field.

EXPERIMENTAL

The dielectric study was performed in cells with metallic electrodes. Although the use of ITO-coated glass plates allows a simultaneous optical control of the alignment, the relaxation associated with the high resistance value of this type of electrode could mask some of the contributions.

Complex dielectric permittivity has been measured with two different impedance analyzers: the HP4191A for the 10^6–10^9 Hz range and the HP4192A for the 10^2–10^6 Hz range. The former measures the impedance of the sample from the reflection coefficient at the end of a 50 Ω coaxial transmission line. In order to guarantee the same alignment conditions in the whole frequency range the same cell must be used for both frequency ranges. Thus, the cell consists of two golden brass electrodes (diameter 3 mm) separated by two 50 μm thick silica spacers, making a plane capacitor located at the end of the line. We used as sample holder a modified HP16091A coaxial test fixture. This was adapted by a connector which allows us to go from APC7 to four wires, with a residual capacity of 2.5 pF, in order to perform measurements with the low frequency analyzer. The sample holder was held in a cryostat, which screens the system, and both temperature and dielectric measurements were fully computer controlled.

Once the specimen was in the cell, it was heated into the isotropic phase and then slowly cooled down to the different mesophases. The electrodes were treated with PVA in order to achieve planar alignment.

RESULTS AND DISCUSSION

The compound has the phase sequence:

C-(56°C)-SmC*-(77.7°C)-SmA-(91.9°C)-N*-(97.3)-I

The chemistry of this material together with calorimetric and spontaneous polarization measurements ($P_{smax} \cong 100\,\mathrm{nC\,cm^{-2}}$) have been published previously.[15]

The transition temperatures have been deduced from texture changes seen using the polarizing microscope and are in accordance with the results of the dielectric study as can be seen in Figure 1, where the dielectric permittivity at 250 Hz for 0 V and 35 V bias voltage has been plotted. At 0 V, a sharp increase at the SmA-SmC* transition, due to the helical structure, is observed. When the bias is on this contribution is quenched and only a little cusp due to the soft mode remains. Although a shift in the para-aferroelectric phase transition is expected, in materials with high spontaneous polarization we assumed as T_C that deduced from the maximum of the soft mode strength at 35 V bias voltage. The small peak superimposed to the broad increase of the Goldstone in the results without bias, could not be clearly assigned to the Goldstone or to the soft mode. The other phase transitions appear as small anomalies.

Before discussing our results, we shall describe some molecular and geometric parameters. We will consider molecules with a dipole moment $\mu = \mu_l + \mu_t$, where μ_l stands for the component of the dipole moment along the molecular long axis and μ_t for the transverse component. The applied electric field is parallel to the smectic layers. We will assume that in the SmC* phase the smectic layers remain approximately perpendicular to the electrodes with the helix axis perpendicular to the electric field.

When performing a frequency scan, the dielectric spectroscopy is able to distinguish among possible molecular motions, whenever they can be coupled with the electric

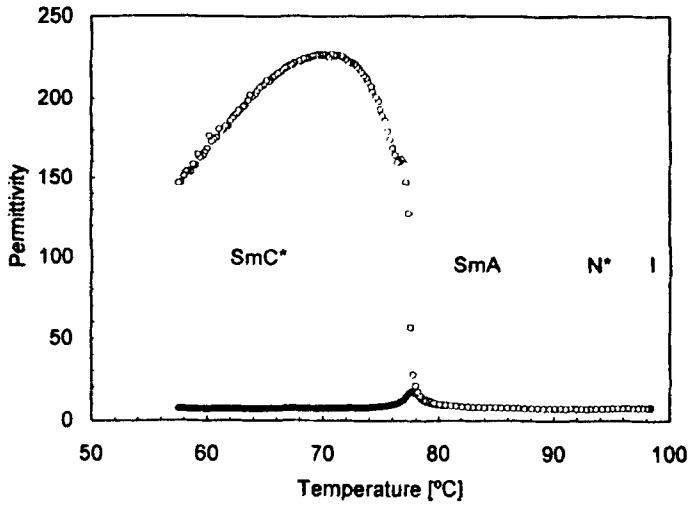

FIGURE 1 Dielectric permittivity, ε' at 250 Hz in the planar alignment: open circles, Vbias = 0 V; dots, Vbias = 35 V.

field, and to separate their contributions to the dielectric permittivity, because of their different characteristic frequencies and, in general, important dipole moments. With this aim, the complex permittivity was measured between 10^2 and 10^9 Hz for all phases. The measurements have been performed under two different bias values 0 V and 35 V. The measurements show that different separated relaxations with different strength, frequency and temperature behaviour are present from the isotropic to the SmC* phase.

Figure 2 shows both components of the complex dielectric permittivity versus the logarithm of the frequency for a temperature in the N* phase. In the I phase the plot is similar. In both phases an important DC conductivity contribution to the losses can be observed. The fact that in the isotropic phase two different relaxations occur allows us to consider two independent motions for the molecule. The high frequency relaxation is mainly related to the rotation around the molecular long axis and then to the transverse dipole moment. The low frequency one is related to the reorientation of the long molecular axis.[16–18] On the other hand, the strength of the high frequency contribution is larger than that of the low frequency one and so we can assume that the transverse dipole moment is larger than the longitudinal one as was expected for a material with a noticeable spontaneous polarization in the ferroelectric phase and could be deduced from the structure of the molecules of the compound.[15]

In the smectic mesophases, with planar alignment, the relaxational pattern changes drastically. More relaxations are present. These additional relaxations are structural modes. In the SmA* phase, the soft mode, related to tilt fluctuations, appears in the low frequency side and the mode related to the rotation around the long axis in the high frequency side. If the order parameter of the longitudinal axis were unity, no contribu-

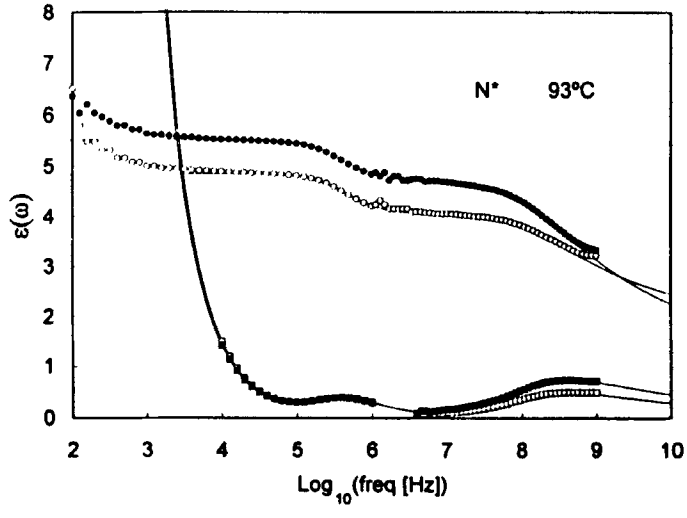

FIGURE 2 Complex permittivitty versus the logarithm of the frequency in the N^* phase: ε'(dots), ε''(squares); white symbols, V bias = 0 V; black symbols, V bias = 35 V. The low frequency relaxation is related to the longitudinal dipole moment and the high frequency relaxation to the transverse dipole moment. Continuous lines: fittings to Equation 1.

tion associated with μ_l could be seen. In any case, it shall be hidden by the soft mode. Figure 3 shows a typical plot of the complex permittivity versus the logarithm of the frequency, for a temperature in the SmA* phase.

In the tilted smectic mesophase, SmC*, the spectrum is a little more complicated. Together with the modes in the orthogonal smectic mesophase, there is a contribution related to the helical structure, the Goldstone mode, whose strength can hide the soft mode. Because of this fact, it is usual to study the dielectric response under a bias field high enough to unwind the helical structure and quench the Goldstone mode. Figure 4 shows a typical plot of the complex permittivity versus the logarithm of the frequency, for a temperature in the SmC* phase far from the SmC*-SmA phase transition. The data without bias field show two relaxations. The high frequency one is related to the rotation around molecular long axis and the low frequency one is the Goldstone mode. When a high enough DC field is applied, the helix unwinds and the Goldstone mode contribution disappears; other possible and smaller relaxations could then emerge. For temperatures near the SmA phase the soft mode is usually observed. For the selected temperature in Figure 4 the spectral shape of the permittivity together with the temperature dependence of the parameters of the relaxation show that this is not the case. The low frequency relaxation must be assigned to some structural process. We shall come back to this point later.

In the isotropic and chiral nematic mesophases, the results were fitted to:

$$\varepsilon(\omega) = \Delta\varepsilon_l(\omega) + \Delta\varepsilon_t(\omega) + \varepsilon_\infty - i\sigma_{DC}/\omega \tag{1}$$

where $\Delta\varepsilon/(\omega)$ stands for the contribution due to the mechanism relaxing in the low frequency side of the scanned spectrum, $\Delta\varepsilon_t(\omega)$ for the high frequency one, ε_∞ for the

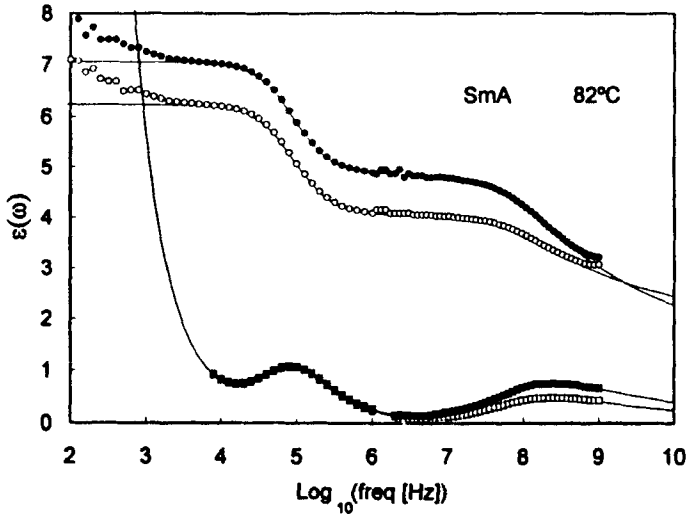

FIGURE 3 Complex permittivitty versus the logarithm of the frequency in the SmA phase: ε' (dots), ε'' (squares); white symbols, Vbias = 0V; black symbols, Vbias = 35V. The high frequency relaxation is related to the transverse dipole moment and the low frequency relaxation to the soft mode. Continuous lines: fittings to Equation 3.

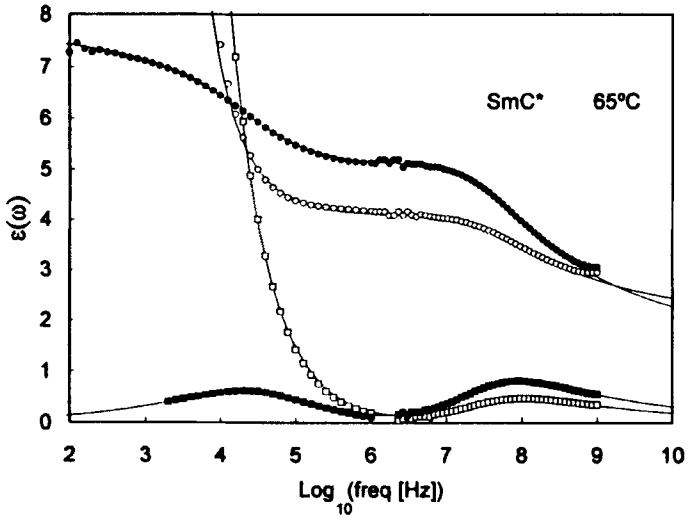

FIGURE 4 Complex permittivitty versus the logarithm of the frequency in the SmC* phase: ε'(dots), ε''(squares); white symbols, Vbias = 0 V; black symbols, Vbias = 35 V. The high frequency relaxation is related to the transverse dipole moment and the low frequency relaxation to Goldstone mode without bias and to the ferroelectric domain mode with Vbias = 35 V. Continuous lines: fittings to Equations 5 and 6.

residual high frequency permittivity after the relaxation of both and σ_{DC} for the conductivity. Both relaxations were fitted to the Havriliak–Negami equation[19] ($j = t, l$):

$$\Delta\varepsilon_j(\omega) = \Delta\varepsilon_j \left\{ \frac{1}{\{1 + (i\omega\tau)^{\alpha}\}^{\beta}} \right\} \tag{2}$$

$\Delta\varepsilon_t$ stands for the strength of the high frequency mechanism. Its frequency of maximum loss is about 1 GHz in the isotropic phase and shows thermal activation. These values together with the activation energy allowed us to assign it to the rotations around molecular long axis. It can be observed along all mesophases, as we shall show below. The low frequency relaxation was fitted to the same equation. Its frequency of maximum losses is about 2 MHz in the isotropic phase and shows an anomalous large thermal activation. It is related to the molecular reorientation around molecular short axis. In the smectic mesophases with planar geometry the dielectric strength of this mode must be very small and so hidden by the structural relaxations. The β parameter takes count of the asymmetry of the relaxation and both, α and β, of the width;[19] when $\alpha, \beta = 1$ the relaxation becomes a Debye relaxation. Table I shows the values of α and β for both relaxations in the different phases. It is worth pointing out that although they are quite different for each relaxations, the parameters of each one do not change much with temperature. The spectral shape of the low frequency relaxation is near Debye-like and the high frequency one is broader, indicating that it could be the result of different molecular motions with similar characteristic frequencies.[20]

TABLE I
Fitting parameters according (2), (4) and (6)

BIAS/V	PHASE	α	β
Rotation around long axis		(*Equation 2*)	
0	I	0.9	0.26
0	N*	0.9	0.26
0	SmA	0.9	0.26
0	SmC*	0.95	0.26
35	N*	0.86	0.26
35	SmA	0.88–0.9	0.26
35	SmC*	0.92–0.95	0.26–0.27
Rotation around short axis		(*Equation 2*)	
0	I	0.91	0.95
0	N*	0.91–0.96	0.95–0.98
Soft mode		(*Equation 4*)	
0	SmA	0.88–0.93	–
35	SmA	0.89–0.92	–
35	SmC*	0.88–0.93	–
Domain mode		(*Equation 6*)	
35	SmC*	0.28	0.5–0.6

In the SmA phase, the results were fitted to:

$$\varepsilon(\omega) = \Delta\varepsilon_s(\omega) + \Delta\varepsilon_t(\omega) + \varepsilon_\infty - i\sigma_{DC}/\omega \tag{3}$$

where $\Delta\varepsilon_s(\omega)$ stands for the contribution due to the relaxation mechanism in the low frequency side of the scanned spectrum. This relaxation was also fitted to the Havriliak–Negami equation, always giving $\beta = 1$. In this case the relaxation is called Cole–Cole and the shape of the dielectric loss is symmetric:[19]

$$\Delta\varepsilon_s(\omega) = \frac{\Delta\varepsilon_s}{1 + (i\omega\tau)^\alpha} \tag{4}$$

with α ranging between .88 and .93. The quantity $\Delta\varepsilon_s$ is the strength of this contribution. The temperature dependence of its frequency of maximum loss and strength allowed us to assign it to the soft mode.

In the SmC* phase, the results were fitted to:

$$\varepsilon(\omega) = \Delta\varepsilon_G(\omega) + \Delta\varepsilon_t(\omega) + \varepsilon_\infty \tag{5}$$

where $\Delta\varepsilon_G(\omega)$ stands for the Goldstone mode contribution. Its amplitude is about 200 and its frequency about 400 Hz in most parts of this mesophase.

When the material is under a bias field, the helix becomes unwound and the Goldstone mode is suppressed. In the first two degrees below the SmA phase, the data were fitted to equation (3). When the temperature decreases from T_C, the frequency of maximum loss first increases, as is expected for the soft mode. After three degrees the

spectral shape of the low frequency relaxation changes from Cole–Cole to inverted Havrilliak–Negami,[19] the frequency stops raising and after begins to decrease. The strength rests almost constant. It should be related to the domain mode described in references 21–23. This domain mode was fitted to:

$$\Delta\varepsilon_D(\omega) = \Delta\varepsilon_D\left[1 - \left\{\frac{(i\omega\tau)^{1-\alpha}}{\{1+(i\omega\tau)^{1-\alpha}\}}\right\}\right] \tag{6}$$

As can be seen in Figures 2, 3 and 4, the amplitude of the high frequency mode is larger when the bias is applied. By contrast, neither the strength of the soft mode (in the SmA phase) nor the strength of the mode associated with the longitudinal dipole depend noticeably on the bias.

From the fittings of the complex permittivity (continuous lines in all figures) we deduced the strengths and frequencies of all mentioned modes. Let us start with the soft mode. Figure 5 shows $1/\Delta\varepsilon_s$ versus temperature and in Figure 6 one can see its relaxation frequency in a plot of log(frequency) versus temperature. Both quantities show the behaviour most frequently observed for the great majority of compounds[1–4,7,8] and that could be described by the classical Landau model for the SmA-SmC* phase transition.[24,25] Nevertheless, for describing other material properties such as the ratio P/θ (spontaneous polarization/molecular tilt) in a better way, the so-called extended model was developed.[26–28] In this model a biquadratic coupling between P and θ is introduced to account for the non-constant value of the ratio P/θ, in fact usually observed and which also affects the behavior of $\Delta\varepsilon_s$ just below the phase transition temperature.[2–4] In our case, this biquadratic coupling must be small. It is important to notice that in this type of study, a strong bias field is applied to the sample

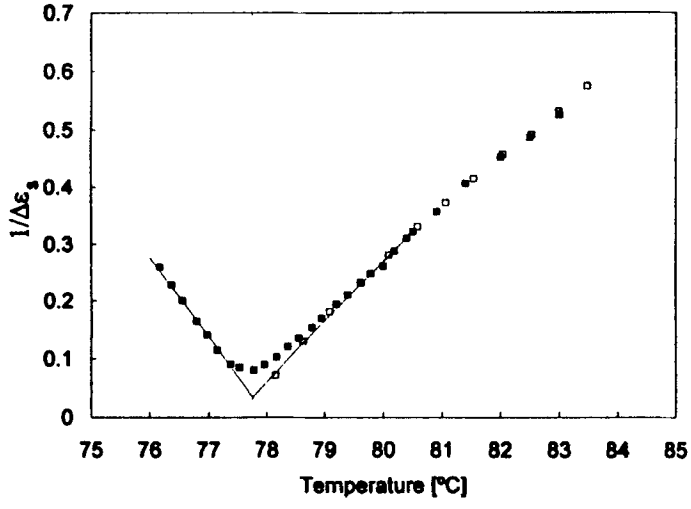

FIGURE 5 Inverse of the soft mode dielectric strength versus temperature: white symbols, Vbias = OV; black symbols, Vbias = 35V. Continuous line show the criterium used to determine de SmA-SmC* transition temperature.

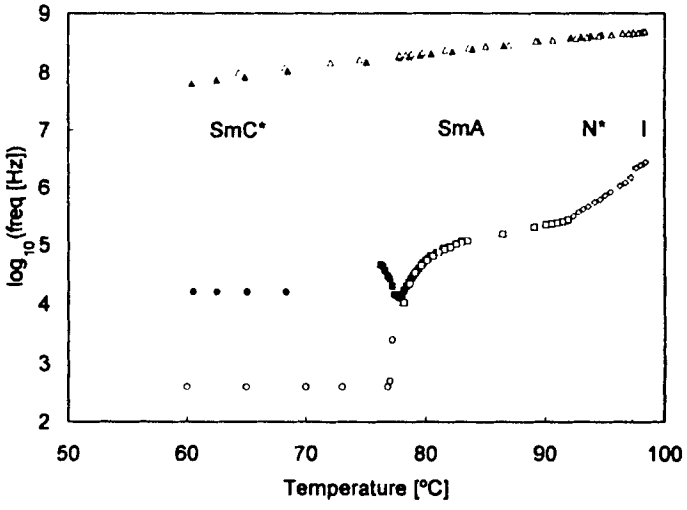

FIGURE 6 Characteristic frequencies of the different modes versus temperature. White symbols, Vbias = 0V; black symbols, Vbias = 35V. (Δ) and (▲) relaxation related to the transverse dipole moment; (◇) relaxation related to the longitudinal dipole moment; (□) and ■ soft mode; (○) Goldstone mode; (●) domain mode.

and this could cause important changes in the behaviour.[1,7] In reference 1 it is shown, for a compound with large soft mode dielectric strength, that its frequency with and without bias is quite different. A similar analysis in the present case was not possible because just below the phase transition Goldstone and soft mode frequencies are very close.

In Figure 7 we have represented the strength of the modes other than the soft and the Goldstone. The relaxation related to the longitudinal dipole moment can be seen in the isotropic and N* phases. Its amplitude is not affected by the bias field and this last case is not represented. It shows a small decrease when going from the isotropic to the N^* phase (due to the planar alignment). In Figure 8 we have represented its characteristic frequency versus temperature in an Arrhenius plot. There is a jump at the I-N^* transition, in fact very frequent for this mode and due to the nematic order. This motion is hindered by the nematic potential. The high value of the activation energy (three times the usually obtained for this motion in most part of compounds), 338 kJ mol^{-1} in the isotropic phase and 353 kJ mol^{-1} in the N^* is noteworthy. These high values could be related to the molecular shape with a branched tail.[15] As we have above mentioned this motion is practically not detectable by dielectric measurements in planar smectic mesophases.

In Figure 7 we also shown the amplitude of the mode detected in the SmC* phase with the helix unwound. Recently, different authors[1,21–23] reported the existence of dielectrically-active processes that could be related to the presence of a modulated structure in the ferroelectric phase. This should be related (in unwound samples) to the breakup of the homogeneous-planar geometry (with tilted smectic layers) into ferroelectric domains for materials with high spontaneous polarization, in a similar way to what happens in solid ferroelectrics to minimize the free energy. *The tilted smectic layers should be ordered as a system of domains and dislocation walls in between with*

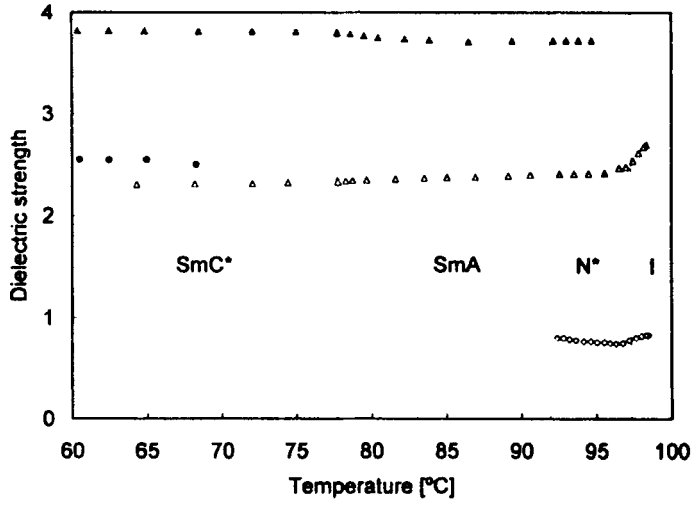

FIGURE 7 Temperature dependence of the dielectric strength of the modes other than soft and Goldstone. Symbols as in Figure 6.

different inclinations of smectic layers and a slight divergence of the spontaneous polarization in the neighbour domains.[23] Two different modes, depending on the localization of the charge involved, are reported: a surface mode and a bulk mode. In our case the bias could be high enough to suppress the last one, so that only the surface domain mode is observed. Characteristic frequencies are similar to those reported.[21–23]

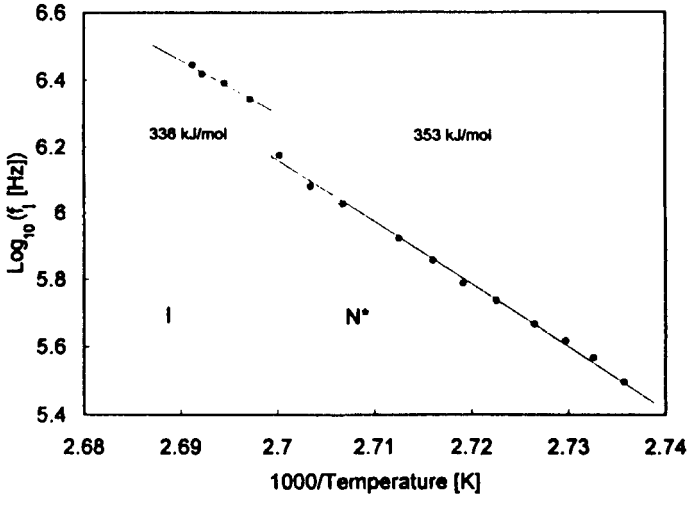

FIGURE 8 Arrhenius plot of the frequency of the mode related to the longitudinal dipole moment.

In Figure 7 we have represented by white triangles the strength of the high frequency mode without bias field ($\Delta\varepsilon_{to}$) and by black triangles with bias field ($\Delta\varepsilon_{t35}$). The value and the temperature dependence of ($\Delta\varepsilon_{to}$) and ($\Delta\varepsilon_{t35}$) are quite different. At 0 V bias field it is almost constant excluding a decrease from the I to the N^* phase, with no discontinuities and no changes in the other phase transitions. At 35 V bias field the strength is much larger and its temperature behaviour is different. It is constant along the N^* phase and at the start of the SmA phase. A few degrees before the SmC* phase it increases until after some degrees in this phase it stabilizes. At this point let us say that all fittings of this mode have been performed with the same α and β parameters. Due to the broad shape of this relaxation, small changes in these parameters cause large changes in the "fitted amplitude". Then, on fitting, we have prime do not change these parameters. In Figure 9 we have represented its characteristic frequency versus temperature in an Arrhenius plot. No jumps, no important changes in the activation energy can be observed. At 0 V the activation energies are slightly different in the different phases: 50 kJ mol^{-1} in the SmC*, 48 kJ mol^{-1} in the SmA, and 53 kJ mol^{-1} in the N^*. At 35 V this energy is 58 kJ mol^{-1} in all phases. Regarding the results in the absence of a bias field in this compound we have obtained what is expected: namely that the characteristics of the molecular motion around the molecular long axis do not change basically nor in the nematic-smectic transition neither in the paraelectric (SmA)-ferroelectric (SmC*) transition, indicating that the appearance of the spontaneous polarization is not related to the freezing of this mode.[9-12,14] When the bias is on, the related motion is more hindered (the activation energy is larger) but more *effective* due to the order imposed by the electric field in the transverse dipole moment: the electric field would act in the same sense as the chiral term in the microscopic model of reference 28.[28] Some controversy exists related to whether this relaxation is or is not related to the two polarization modes predicted by the mean field theory.[26,27] Taken into account that this relaxation is quite broad due to the contributions of the librations of

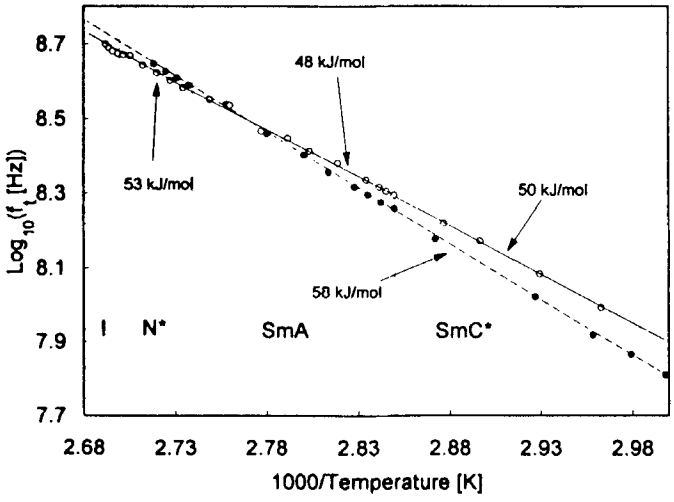

FIGURE 9 Arrhenius plot of the frequency of the mode related to the transverse dipole moment.

the long molecular axis[29] and that the predicted splitting when going into the SmC* phase must be very little,[30] we think that the dielectric measurements are not able to distinguish between one or two processes (as it should be according to the Landau theory). The related frequency do not show any slowing down and as its value is similar in non-chiral smectogens,[17] then it seems unreasonable to relate it to the polarization modes of the Landau theory.

Summarizing, we have performed dielectric measurements between 10^2 and 10^9 Hz on a planar-aligned ferroelectric liquid crystal. Together the soft and Goldstone modes an additional mode related to ferroelectric domains have been detected in the SmC* phase. Relaxations related to rotations around the molecular short and long axes have also been characterized.

Acknowledgement

This work was supported by the CICYT (MAT-91-0962-C02-02) and the EC Human Capital and Mobility Programme (ERB4050 PL922749).

References

1. J. Zubia, A. Ezcurra, M. R. de la Fuente, M. A. Pérez Jubindo, T. Sierra, J. L. Serrano. *Liq. Cryst.*, **10**, 849 (1991).
2. A. Ezcurra, M. A. Pérez Jubindo, M. R. de la Fuente, J. Etxebarria, A. Remón, M. J. Tello, *Liq. Cryst.*, **4**, 125 (1989).
3. M. R. de la Fuente, A. Ezcurra, M. A. Pérez Jubindo, J. Zubia, *Liq. Cryst.*, **7**, 51 (1990).
4. F. Gouda, T. Carlsson, G. Andersson, S. T. Lagerwall, B. Stebler, *Liq. Cryst.*, **16**, 315 (1994).
5. C. Legrand, J. Parneix, *J. Phys., France*, **51**, 787 (1990).
6. A. M. Biradar, S. Wrobel, W. Haase, *Phys. Rev. A*, **39**, 2693 (1989).
7. M. Glogarová, J. Pavel, *Liq. Cryst.*, **3**, 325 (1989).
8. F. Gouda, K. Skarp, S. T. Lagerwall, *Ferroelectrics*, **113**, 165 (1991).
9. M. R. de la Fuente, M. A. Pérez Jubindo, J. Zubia, T. Pérez Iglesias, A. Seoane, *Liq. Cryst.*, **16** (1994) (in press).
10. F. Kremer, A. Schönfeld, S. U. Vallerien, A. Hofmann, N. Schwenk, *Ferroelectrics*, **121**, 13 (1991).
11. A. Schönfeld, F. Kremer, R. Zentel, *Liq. Cryst.*, **13**, 403 (1993).
12. F. Kremer, S. U. Vallerien, H. Kapitza, R. Zentel, E. W. Fischer, *Phys. Rev. A*, **42**, 3667 (1990).
13. J. R. Lalanne, C. Buchert, D. Destrade, H. T. Nguyen, J. P. Marcerou, *Phys. Rev. Lett.*, **62**, 3046 (1989).
14. J. P. O'Brien, T. Moses, W. Chen, E. Freysz, Y. Ouchi, Y. R. Shen, *Phys. Rev. E*, **47**, R2269 (1993).
15. T. Sierra, M. B. Ros, A. Ezcurra, J. Zubia, *J. Am. Chem. Soc.*, **114**, 7645 (1992).
16. H. Kresse, *Advances in Liquid Crystals*, Vol. 6, (Academic Press), Pg 109 (1983).
17. C. Druon, J. M. Wacrenier, *Mol. Cryst. Liq. Cryst.*, **108**, 291 (1984).
18. A. Kozak, J. K. Moscicki, G. Williams, *Mol. Cryst. Liq. Cryst.*, **201**, 1 (1991).
19. C. J. F. Böttcher, P. Bordewijk, *Theory of Electric Polarization*, Vol. 2, edited by Elsevier Publishing Company, Chap. 9 (1978).
20. A. Jákli, A. Buka, *KFKI-1984-23 Hungarian Academy of Sciences.*
21. L. A.. Beresnev, M. Pfeiffer, S. Pikin, W. Haase, L. Blinov, *Ferroelectrics*, **132**, 99 (1992).
22. W. Haase, S. Hiller, M. Pfeiffer, L. A. Beresnev, *Ferroelectrics*, **140**, 37 (1993).
23. S. A. Pikin, L. A. Beresnev, S. Hiller, M. Pfeiffer, W. Haase, *Journal*, **3**, 1 (1993).
24. S. A. Pikin, V. L. Indebom, *Ferroelectrics*, **20**, 151 (1978).
25. R. Blinc, B. Zeks, *Phys. Rev. A*, **18**, 740 (1978).
26. T. Carlsson, C. Filipic, I. Levstik, B. Zeks, *Phys. Rev. A*, **35**, 3527 (1987).
27. T. Carlsson, B. Zeks, C. Filipic, A. Levstik, *Phys. Rev. A*, **42**, 877 (1990).
28. B. Urbanc, B. Zeks, *Liq Cryst.*, **5**, 1075 (1989).
29. C. M. Haws, M. G. Clark, G. S. Attard, in *Side Chain Liquid Crystal Polymers* (Ed: C. B. McArdle), Blackie, Glasgow 1989, Ch. 7.
30. P. G. Costello, Yu. P. Kalykov, J. K. Vij, *Phys. Rev. A*, **46**, 4852 (1992)..